

## COMPUTATIONAL ANALYSIS OF ENTROPY GENERATION IN A COUPLE STRESS FLUID FLOW THROUGH A VERTICAL POROUS MEDIUM

*Akaje T.W.*

Department of Mathematics, Federal University of Agriculture, Abeokuta, Nigeria

### *Abstract*

---

*The paper investigates computational analysis of entropy generation in a couple stress fluid flows through a vertical porous channel occupied with saturated porous materials. Semi-analytical solutions of the dimensionless momentum and energy equations are derived using differential transform method. The entropy generation, irreversibility distribution ratio and the Bejan number in the flow field were computed through the approximate solution. The effects of various flow physical parameters on the velocity and temperature are discussed and represented graphically.*

---

**Keywords:** Entropy generation, Couple Stress, Porous Vertical channel and porous media.

### **1.0 Introduction**

Reasonable attention has been given on how to control or minimize energy wastages in form of heat dissipation when energy is generated. And this was done because of their numerous physical applications in industrial engineering processes. Numbers of research work on the minimization of entropy generation has been spurred, especially when dealing with heat transfer problem. In [1] developed the method for minimizing entropy generation rate in irreversible processes.

Studied [2] entropy generation in the laminar natural convection from a constant temperature vertical plate in an infinite fluid. Entropy generation in a porous channel with hydromagnetic effects was investigated by [3]. The study of entropy generation in a liquid film falling along an inclined porous heated plate reviewed by [4]. Analysis of entropy generation and thermal stability in a slab was also studied by [5]. In [6] entropy generation under the effect of suction/injection was investigated and observed that entropy generation is higher near the cold stationary porous plate in comparison to the hot moving porous plate. It is also noticed in the same paper that entropy generation number increase in the injection.

The combined effect of buoyancy force and Navier slip on entropy generation in a vertical porous channel was investigated by [7]. The findings of their works show that there is little restrictive medium at the injection walls and more restrictive medium at the suction walls. The effect of couple stresses on entropy generation rate in a porous channel with convective heating was examined in [8] and reported that, an increase in the couple stress inverse is observed to increase the entropy generation rate at the plate with Newtonian heating while the entropy generation decreases with an increase in the couple stress inverse at the wall with Newtonian cooling. Effect of convective heating on entropy generation rate in a channel with permeable walls cited by [9] and it was reported that increase in Reynolds numbers decrease Bejan number at the lower wall region and increase Bejan number at the upper region. Heat transfer irreversibility dominates the centerline region of the channel was also observed. In [10] effects of radiation heat transfer on entropy generation at thermosolutal convection in a square cavity subjected to a magnetic field was investigated and the same results with others researchers about entropy generation increases with radiation parameter but it decreases with Hartmann number and total entropy generation is influenced by the buoyancy ration, a minimum is observed for  $N = -1$ .

More so several researchers have studied the effect of couple stress flow in entropy generation in recent time like [11] Second law analysis for third-grade fluid with variable properties was studied. Effect of couple stress on the flow in a constricted annulus was investigated by [12], reported the second law analysis for hydromagnetic couple stress fluid flow through a porous channel. Irreversibility analysis of a radiation MHD poiseuille flow through a porous medium with slip condition in [13], examined. Entropy generation of double-diffusive convection in the presence of rotation reported in [14]. Investigation of irreversibility analysis in a couple stress film flows along an inclined heated plate with the adiabatic free surface observed by [15]. Entropy generation of turbulent double-diffusive natural convection in a rectangle cavity was analyzed by [16]. The second law analysis for a porous channel flow with asymmetric slip and convective boundary conditions was investigated by [17].

---

Corresponding Author: Akaje T.W., Email: akajewasiu@gmail.com, Tel: +2348035568269

In [18] Entropy generation due to MHD flow in a porous channel with Navier slip was observed. Entropy generation in couple stress fluid flow through the porous channel with slippage was investigated by [19]. Second law analysis for variable viscosity hydro magnetic boundary layer flow with thermal radiation and Newtonian heating analyzed by [20]. They all have a similar report about the effect various parameters on entropy generation profile.

To the best knowledge of the authors/researchers, the buoyancy effect on the inherent irreversibility in a couple stress fluid flows through vertical porous channels packed with saturated porous media has not been reported yet in the literature.

This paper analyzes computational analysis of entropy generation in a couple stress fluid flows through a vertical porous channel with suction and injection packed with saturated porous media in the presence of buoyancy force is investigated numerically, using differential transform method. Both numerical and graphical results for velocity, temperature, entropy generation rate and Bejan number are presented and discussed quantitatively with respect to various parameters embedded in the system.

MATHEMATICAL FORMULATION

d

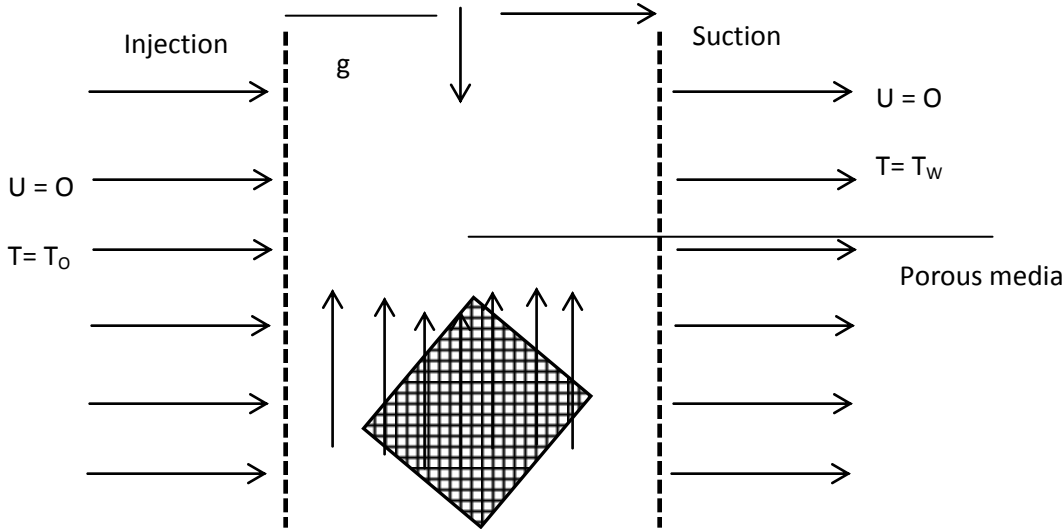


Figure 1 Geometry of the problem

Consider the steady laminar flow of an incompressible couple stress fluid through vertical porous channels of distance  $d$  apart packed with porous media as shown above. The left channel wall is subjected to injection of fluid while the right is subjected to suction with constant velocity.  $T_w$  and  $T_o$  represent the temperature of two sides of the walls, in which the  $T_w$  is greater than  $T_o$ . The density variation due to buoyancy effect is taken into consideration in the momentum equation using a Boussinesq approximation. Following [11], [16], the momentum and energy equations are given below:

$$\rho v_o \frac{du^*}{dy^*} = -\frac{dp}{dx} + \mu \frac{d^2u^*}{dy^{*2}} - \delta \frac{d^4u^*}{dy^{*4}} - \frac{\mu u^*}{k} + g\beta(T - T_o) \tag{1}$$

$$\rho C_p \frac{dT^*}{dy^*} = k \frac{d^2T^*}{dy^{*2}} + \mu \left(\frac{du^*}{dy^*}\right)^2 + \delta \frac{d^2u^*}{dy^{*2}} + \frac{\mu u^{*2}}{k} + \frac{cu^{*3}}{\sqrt{k}} \tag{2}$$

With

$$u^* = \frac{d^2u^*}{dy^{*2}} = 0, T^* = T_o \text{ on } y = 0 \tag{3}$$

$$u^* = \frac{d^2u^*}{dy^{*2}} = 0, T^* = T_w \text{ on } y^* = h \tag{4}$$

Where  $u$  is the axial velocity,  $d$  is the channel width,  $\mu$  is the dynamic viscosity,  $\rho$  is the fluid density,  $T$  is the fluid temperature,  $C_p$  specific heat at constant pressure,  $k$  is the thermal conductivity of the fluid,  $k$  is the porous media permeability,  $c$  is the empirical constant in the second order resistance such that  $c = 0$  corresponds to the Darcy law,  $\delta$  is the fluid particle size effect due to couple stresses. Introducing the following dimensionless variables.

$$\eta = \frac{y^*}{h}, w = \frac{u^* h \rho}{\mu}, \theta = \frac{T^* - T_o}{T_w - T_o}, X = \frac{x}{h}, A = \frac{-dp}{dx}$$

$$Pr = \frac{\mu C_p}{K}, p = \frac{h^2 \rho p}{\mu^2}, S = \frac{h^2}{K}, M = \frac{ch}{\rho \sqrt{k}}, \lambda = \frac{\delta}{\mu h^2}$$

$$Gr = \frac{g\beta \rho h^3 (T_w - T_o)}{\mu^2}, Br = \frac{V_o^2 \mu}{k(T_w - T_o)}, Ns = \frac{T_o^2 h^2 EG}{k(T_w - T_o)^2}$$

$$\Omega = \frac{T_w - T_o}{T_o}, \quad Ec = \frac{\mu^2}{\rho^2 h^2 Cp(T_w - T_o)}, \quad Ks = \frac{V_o h}{V} \quad (5)$$

Putting equation (5) into equations (1)- (4) we have the dimensionless governing equations as:

$$K_s \frac{dw}{d\eta} = A + \frac{d^2 w}{d\eta^2} - \frac{\lambda d^4 w}{d\eta^4} - Sw - mw^2 + Gr\theta \quad (6)$$

$$K_s Pr \frac{d\theta}{d\eta} = \frac{d^2 \theta}{d\eta^2} + Pr Ec \left[ \left( \frac{dw}{d\eta} \right)^2 + \lambda \left( \frac{d^2 w}{d\eta^2} \right)^2 + Sw^2 + mw^3 \right] \quad (7)$$

With the appropriate boundary conditions

$$w = \frac{d^2 w}{d\eta^2} = 0, \theta = 0, \text{ on } \eta = 0 \quad (8)$$

$$w = \frac{d^2 w}{d\eta^2} = 0, \quad \theta = 1 \text{ on } \eta = 1 \quad (9)$$

Here Gr is the grashof number due to buoyancy effect, Ec is the Eckert number, Ks is the suction/Injection Parameter  $\theta$  is the dimensionless temperature, S is the porous media shape factor parameter, M the second order porous media resistance parameter and A is the axial pressure gradient parameter.  $\mu$  is the dimensionless entropy generation rate, Be is the Bejan number, while Pr and Br represent Prandtl and Brinkman numbers,  $\Omega$  is the parameter that measures the temperature difference between the two heat reservoirs and Ks is the suction/injection parameter.

### 3.0 Entropy Generation Analysis

The convection process along a porous wall is naturally irreversible. Exchange of energy and momentum within the fluid and at the solid boundaries causes the non-equilibrium condition, which leads to continuous entropy generation rate in the porous wall. [21] gave a volumetric rate of entropy generation in Cartesian coordinates as:

$$E_G = \frac{k}{T_o^2} \left( \frac{dT^*}{dy^*} \right)^2 + \frac{\mu}{T_o} \left( \frac{du^*}{dy^*} \right)^2 + \frac{\delta}{T_o} \left( \frac{d^2 u^*}{dy^{*2}} \right)^2 + \frac{\mu u^{*2}}{T_o K} + \frac{Cu^{*3}}{T_o \sqrt{K}} \quad (10)$$

Where the first term on the right-hand side of equation (10) is the irreversibility due to heat transfer and the second term is the entropy generation due to viscous dissipation. The third, fourth and fifth terms represent couple stress effect and irreversibility due to the presence of porous media. Using equation (5), equation (10) reduces to

$$Ns = \frac{T_o^2 h^2 EG}{K(T_w - T_o)} = \left( \frac{d\theta}{d\eta} \right)^2 + \frac{Br}{\Omega} \left[ \left( \frac{dw}{d\eta} \right)^2 + \lambda \left( \frac{d^2 w}{d\eta^2} \right)^2 + Sw^2 + Mw^3 \right] \quad (11)$$

Which is the dimensionless form of equation (10)

Where  $\mu = \frac{T_w - T_o}{T_o}$  is the temperature difference parameter and Br = Prec is the Briukmann number.

The Bejan number (Be) is defined as:

$$Be = \frac{N_i}{N_s} = \frac{1}{1+\phi} \quad \text{Where } Ns = N_1 + N_2, N_1 = \left( \frac{d\theta}{d\eta} \right)^2 \text{ Heat transfer irreversibilities}$$

$$N_s = \frac{Br}{\Omega} \left[ \left( \frac{dw}{d\eta} \right)^2 + \lambda \left( \frac{d^2 w}{d\eta^2} \right)^2 + Sw^2 + Mw^3 \right] \quad (12)$$

(Irreversibility due to viscous dissipation, couple stress, and porous media).

$\phi = \frac{N_1}{N_2}$  (Irreversibility ratio).

Where Be= 1 is the unit at which heat transfer irreversibility dominates, Be= 0 is the limit at which fluid friction irreversibility dominates, and Be= 0.5 implies that both of them contribute equally.

### 3.0 The Differential Transform Method.

The differential transform method is a semi-analytical that depends on Taylor series. The concept of differential transformation method was first introduced by [22], to study electrical circuits. The main advantage of this method is that it can be applied directly to nonlinear ordinary and partial differential equations without requiring linearization, discretization or perturbation, it been studied and applied widely during the last two decades. There is tremendous interest in the application of the DTM to solve various scientific problems. For instance, [23], applied differential transform method for some delay differential equations. [24], introduced differential transformations and mathematical modeling of physical processes. [25], studied the application of differential transform method to differential-algebraic equations. [26], studied general differential transformation method for a higher order of linear boundary value problem. [27] Solutions of delay differential equations by using differential transform method. [28], investigated second- law [29], Studied general differential transformation method for a higher order of linear boundary value problem. Using differential transform method and Pade approximant for solving

MHD flow in a laminar liquid film from a horizontal stretching surface was investigation by [30]. Previous studies agreed that the DTM can be easily applied in linear and nonlinear differential equations.

The DTM is developed base on the Taylor series expansion. This method constructs an analytical solution in the form of apolynomial.

Definition 1

A Taylor Polynomial of degree n is defined as follows:

$$P_x(x) = \sum_{k=0}^n \frac{1}{k!} (f^k(c))(x - c)^k \tag{13}$$

**Theorem 1**

Suppose that the function f has (n+1) derivative on the interval (c-r, c+r), for some r>0 and

$\lim_{x \rightarrow \infty} R_n(x) = 0$  for all  $x \in (c-r, c+r)$  where  $R_n(x)$  is the error between  $R_n(x)$  and the approximated function f(x). Then, the Taylor series expanded about x=c converges to f(x).

That is

$$f(x) = \sum_{k=0}^{\infty} \frac{1}{k!} (f^k(c))(x - c)^k \tag{14}$$

For all  $x \in (c - r, c + r)$ .

**Definition 2**

The differential transform of the function F(x) for the K-th derivatives is defined as follows:

$$F(k) = \frac{1}{k!} \left[ \frac{d^k f(x)}{dx^k} \right]_{x = x_0} \tag{15}$$

Where f(x) is the original function and F (k) is the transformed function.

**Definition 3**

The inverse differential transform of F (k) is defined as:

$$f(x) = \sum_{k=0}^{\infty} (x - x_0)^k F(k) \tag{16}$$

Putting equation (14) into equation (15) we have

$$f(x) = \sum_{k=0}^{\infty} (x - x_0)^k F(k) \frac{1}{k!} \left[ \frac{d^k f(x)}{dx^k} \right] \tag{17}$$

This is the Taylor series of f(x) at x= x<sub>0</sub>. The following basic operation of differential transformation can be deduced from equations (14) and (15).

Original function	Transformed function
$f(x) = u(x) \pm v(x)$	$F(K) = U(K) \pm V(k)$
$f(x) = \frac{d^n u(x)}{dx^n}$	$F(K) = \frac{(k+n)!}{k!} U(k+n)$
$f(x) = \lambda u(x)$	$F(K) = \lambda U(K)$
$f(x) = x \frac{du(x)}{dx}$	$F(K) = \sum_{r=0}^k \delta(r-1)(k-r+1)U(k-r+1)$
$f(x) = \frac{xd^2u(x)}{dx^2}$	$F(K) = \sum_{r=0}^k \delta(r-1)(k-r+1)(k-r+2)U(k-r+2)$
$f(x) = \frac{du(x)}{dx} \cdot \frac{du(x)}{dx}$	$F(K) = \sum_{r=0}^k (r+1)(k-r+1)U(r+1)U(k-r+1)$
$f(x) = \frac{d^2u(x)}{dx^2} \cdot \frac{d^2u(x)}{dx^2}$	$F(K) = \sum_{r=0}^k (r+1)(r+2)(r-r+2)(k-r+1)U(r+2)U(r-r+2)$
$f(x) = U(x) \cdot \frac{d^2u(x)}{dx^2}$	$F(K) = \sum_{r=0}^k (k-r+2)(k-r+1)U(r)U(k-r+2)$
$f(x) = 1$	$F(K) = \delta(k)$
$f(x) = x$	$F(K) = \delta(k-1)$

Taking differential transform of (6) - (9) and (11) by the related definitions in

Table 1 above we obtain

$$\begin{aligned}
 K_s(k+1)w(k+1) &= A\delta[k,0] + (k+1)(k+2)w(k+2) \\
 &\quad - \lambda(k+1)(k+2)(k+3)(k+4)w(k+4) \\
 &\quad - Swck - M \sum_{r=0}^k w(r)w(k-r) \\
 K_s Pr(k+1)\theta(k+1) &= (k+1)(k+2)\theta(k+2)
 \end{aligned} \tag{18}$$

$$\begin{aligned}
 &K_s \Pr(k+1) \theta(k+1) \\
 &= (k+1)(k+2)\theta(k+2) \\
 &+ PrEC \left[ \sum_{r=0}^k (k+1)(K-r+1)w(r+1)w(k-r+1) \right. \\
 &+ \lambda \sum_{r=0}^k (r+1)(r+2)(k-r+1)w(r+2)w(k-r) \\
 &\left. + 2s \sum_{r=0}^k w(r).w(k-r) + M \sum_{r=0}^k \sum_{t=0}^r w(t)w(r-t)w(k-r) \right] \tag{19}
 \end{aligned}$$

Also, the transform of boundary conditions gives  $\sum_{k=0}^m w(k) = 0, \sum_{k=0}^m k(k-1)w(k) = 0 \sum_{k=0}^m \theta(k) = 1$  (20)

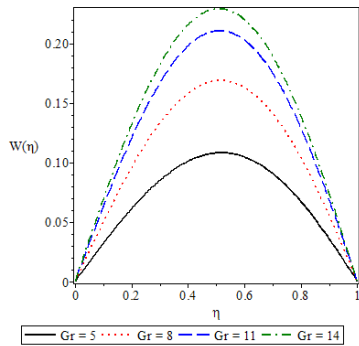
**4. Results and Discussion**

In order to validate our results, we have taken reasonable values for some physical parameters. The Prandtl number was taken in the range of Pr=0.71 to 7.1 which corresponds to Prandtl number in the range of air and that of water. Therefore, the numerical solutions of this problem are performed and the results are illustrated graphically.

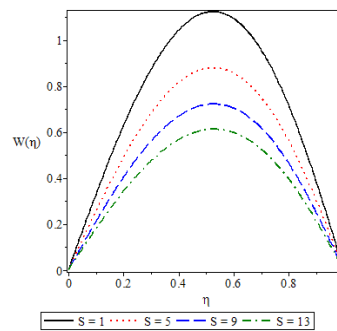
**4.1 Effects of Parameters Variation on Velocity profile**

Figure 2 depicts the effect of an increase in Grashof number (Gr) on the axial velocity profile. And it is observed that the velocity profile increases with increasing Gr. Which shows that the flow accelerates as Gr increases, figures 3 and 4 showed the effect of porous media parameter(s) and couple stress parameter( $\lambda$ ) on the velocity profile. It is observed from these figures that as s and  $\lambda$  are increased, respectively, of the following velocity is decreased. Which shows that the presence of porous media and couple stress parameters in the fluid reduced the rate of fluid flow in the channel. While the velocity of the flow accelerates as Prandtl number increasing in figure 5. But the fluid flow in the channel accelerates largely when Prandtl number is 7.1 . Figure 6 shows an increase in the second order porous media resistance parameter (m) and decreases the velocity profile of the flow. Figure 7 indicated the effect of the axial pressure gradient parameter (A) on the velocity profile. It noticed that an increase in A accelerates the velocity profile of the flow.

Figures 8 and 9 showed the effect of Ecker number (Ec) and Suction/injection parameter (Ks) on the velocity profile. It is noticed from these figures that as Ec and Ks increased, respectively, the velocity of the flow also increased.



**Figure 2:** Effect of increasing Gr on velocity profiles



**Figure 3:** Effect of increasing S on velocity profiles

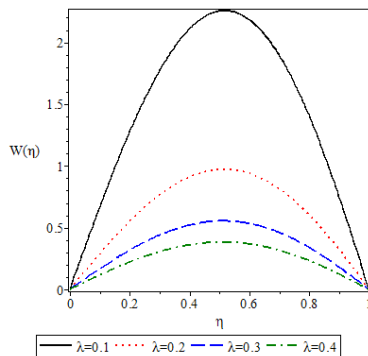


**Figure 4:** Effect of increasing lambda on velocity profiles

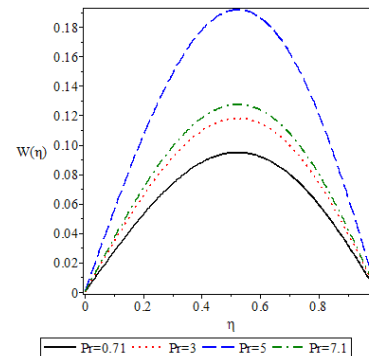


**Figure 5:** Effect of increasing Pron velocity profiles

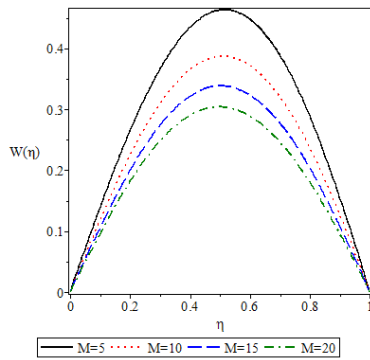


Figure 6: Effect of increasing  $M$  on velocity profiles

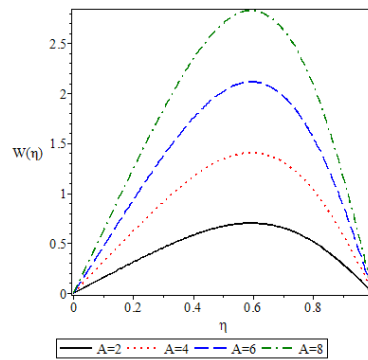


Figure 7: Effect of increasing  $A$  on velocity profiles

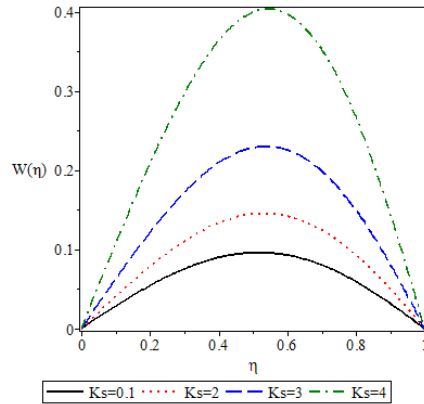


Figure 8: Effect of increasing  $Ks$  on velocity profiles

4.2 Effects of Parameters Variation on Temperature profile

The effect of the variation of parameters on temperature profile is illustrated graphically in figures 10- 16. Figure 10 indicates the effect of  $Gr$  on the temperature profile and it is noticed that increases in  $Gr$  lead to decreases in the temperature profile. The effect of  $s$  on the temperature profile is presented in figure 11. It is observed that an increase in the porous media parameter  $S$  causes a decrease in the temperature. Figures 12 illustrates the effect of couple stress parameter  $\lambda$  on the temperature profile. It is observed from the figures that as  $\lambda$ , increased, the temperature profile decreased and this proves that couple stress will eventually decrease fluid temperature within the channel. While the effect of second order porous media parameter  $M$  on the temperature profile is illustrated in figure 13. It noticed that increase in  $M$  leads to decrease in the temperature profile. Figure 14, it is observed from this figure that fluid temperature increases as  $Pr$  increases. Physically, as the  $Pr$  increases, the thermal diffusivity of the working fluid decreases, so that there is a decrease in the diffusion of the heat generated by viscous dissipation within the channel. consequently, there is an accumulation of heat within the channel leading to increasing in fluid temperature. While the effect of injection/suction parameter  $Ks$  illustrated in figure 15. As this parameter is increasing, it is observed that the temperature of the flow increases. The result shows that, the fluid temperature within the channel accelerates uniformly when more hot fluid is injected into the channel.

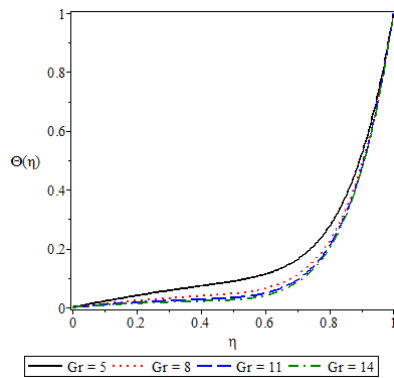


Figure 9: Effect of increasing  $Gr$  on Temperature profiles

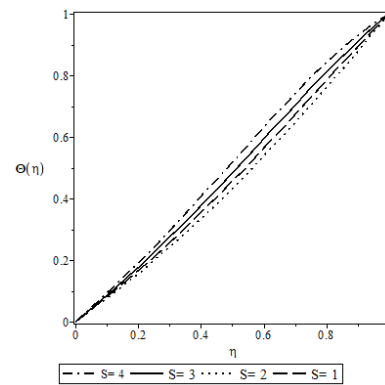


Figure 10: Effect of increasing  $S$  on Temperature profiles

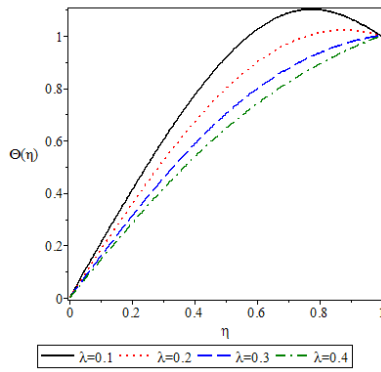


Figure 11: Effect of increasing  $\lambda$  on Temperature profiles

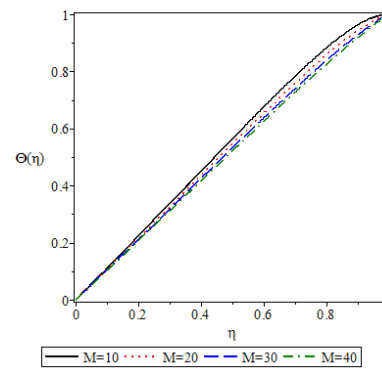


Figure 12: Effect of increasing  $M$  on Temperature profiles

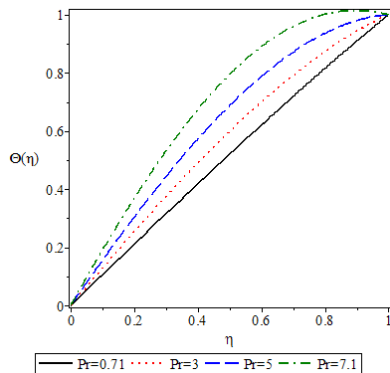


Figure 13: Effect of increasing  $Pr$  on Temperature profiles

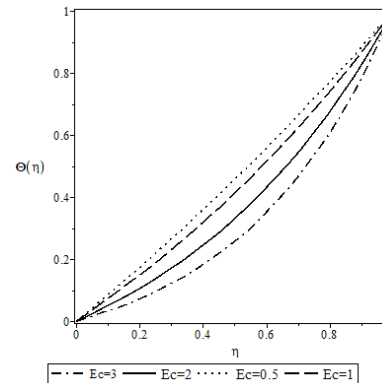


Figure 14: Effect of increasing  $\lambda$  on Temperature profiles

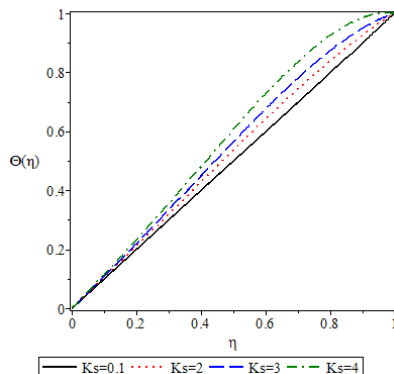


Figure 15: Effect of increasing  $K_s$  on Temperature profiles

### 4.3 Effects of Parameters Variation on Entropy Generation Profiles

The entropy generation profiles for different values of key fluid parameters are illustrated in figures 17----21. Figure 17 illustrates the entropy generation rate when axial gradient pressure ( $A$ ) is increasing, and other parameters remain constant. As  $A$  increases, an increase in entropy production is observed at both walls but the increment in entropy generation is more at the suction wall. Figure 18 shows the effect of Grashof number ( $Gr$ ) on entropy generation when other fluid parameters remain constant. As  $Gr$  number increases, an increase in entropy generation is noticed at both walls but there is a small increase in injection wall. In figure 19, entropy generation rate is observed to decrease with an increase in the couple stress parameter ( $\lambda$ ). The influence of  $\lambda$  on entropy is more pronounced near the suction wall, while the effect diminishes towards the injection wall. The effect of couple stress on the entropy is to lower the entropy generation rate due to rise in the fluid viscosity which reduces the rate of disorderliness of the fluid particles in the center of the channel. It is observed that entropy generation rate decreases as  $S$  increases but large decrease is observed at the suction wall in figure 20. Figure 21, shows the effect of second order porous media resistance parameter, ( $M$ ) on entropy generation when other parameters are kept constant. Increases in  $M$  decrease the entropy generation rate at both walls.

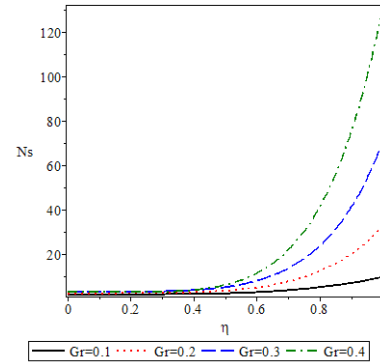
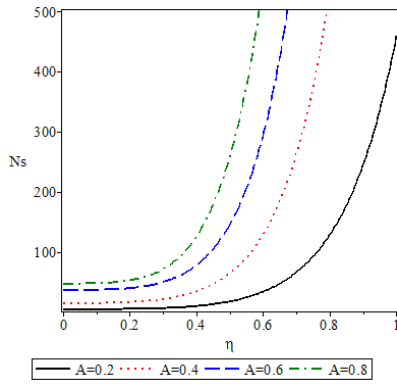


Figure 16: Effect of increasing  $A$  on Entropy generation rate      Figure 17: Effect of increasing  $Gr$  on Entropy generation rate

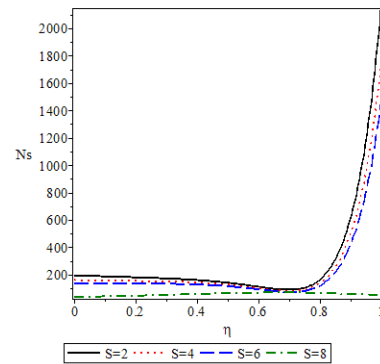
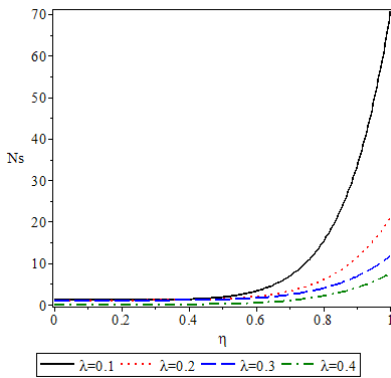


Figure 18: Effect of increasing  $\lambda$  on Entropy generation rate      Figure 19: Effect of increasing  $S$  on Entropy generation rate

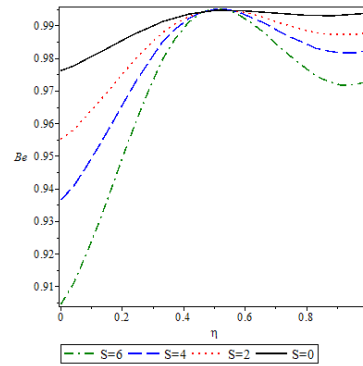
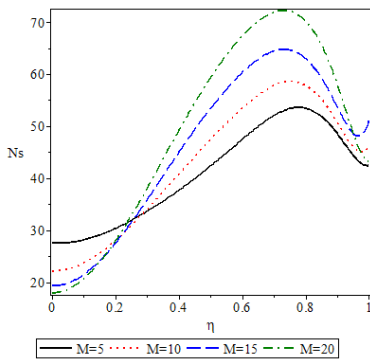


Figure 20: Effect of increasing  $M$  on Entropy generation rate      Figure 21: Effect of increasing  $S$  on Bejan

**4.5 Effects of Parameters Variation on Bejan Number**

The effect of various thermophysical parameters is illustrated in figures 22-27. As  $S$  increases the Bejan number at both wall decreases, while large decrease observed at the injection and small decrease noticed at the suction in figure 22. The figure, 23, shows a large uniform decrease in the Bejan number as  $PrEc$  increases at the lower wall. Figures, 24, 25 show the effect of fluid parameters of  $A$  and  $M$  on the Bejan number. An increase in each of these parameters decreases the Bejan number across the flow uniformly. The effect of the fluid parameter  $\Omega$  on the Bejan number observed in figure 26. An increase in  $\Omega$  increases the Bejan number and there are large increases at the injection wall, While small increase at suction wall observed.



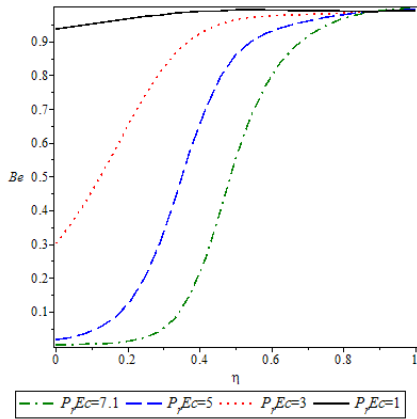


Figure 22: Effect of increasing  $P_r Ec$  on Bejan

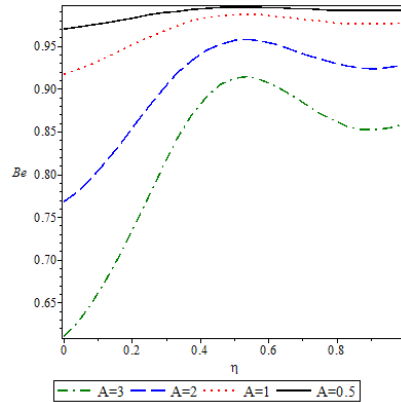


Figure 23: Effect of increasing  $A$  on Bejan

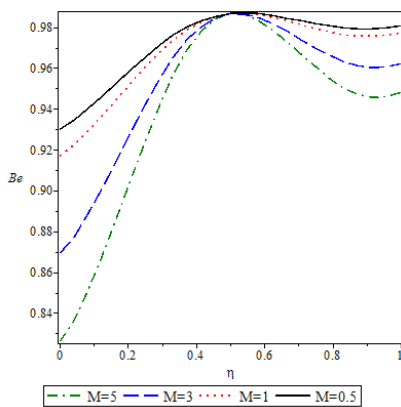


Figure 24: Effect of increasing  $M$  on Bejan

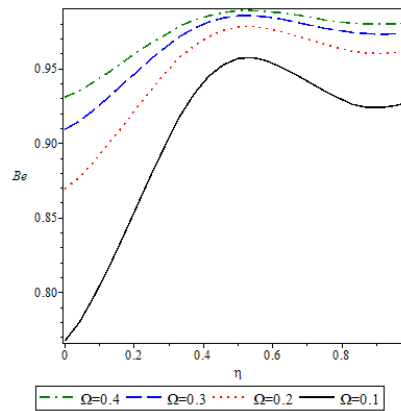


Figure 25: Effect of increasing  $\Omega$  on Bejan

### 5. Conclusions

The entropy generation in couple stress fluid flows through a vertical porous channel packed with saturated porous media was investigated. The analytical solution of the governing momentum and energy equations are obtained using Differential Transform Method. The effect of each of the governing parameters is discussed and illustrated graphically. It is observed that, increase in each of these parameters  $Gr$ ,  $\lambda$ ,  $S$  and  $M$  decrease the temperature profile, while increases in  $Pr$ ,  $Ec$ , and  $Ks$  increase the temperature profile. An increase in  $A$ ,  $Gr$ , and  $\lambda$  increases the entropy generation but the increment in entropy generation is more at the suction wall than injection wall, entropy generation decreases as  $S$  increases but large decreases observed at the suction wall. But entropy generation decreases at both walls as  $M$  increases. Bejan number decreases at both injection and suction walls with increases in  $S$ ,  $A$ , and  $M$ , while Bejan number decreases uniformly at injection wall with increases in  $Pr Ec$ .

### 6. Acknowledgement

The author appreciates the contributions of Professor B.I Olajuwon

### 7. References

- [1] Bejan A. (1996) Entropy generation minimization: the method of thermodynamic optimization of finite-size systems and finite-time processes, CRC Press.
- [2] Ozokol. I, Komurgoz. G, Arikoglu. A.(2007) Entropy generation in the laminar natural convection
- [3] Tasnim, S.H; Mahmud, S.; Mamun, M.A.H.(2002) Entropy generation in a porous channel with hydromagnetic effects. Energy, 2, 300-308.
- [4] Makinde O.D, Osalusi E. (2006) Entropy generation in a liquid film falling along an incline the porous heated plate. Mech Res Commun 33:692-698.

- [5] Aziz A, Makinde O.D. (2010) Analysis of entropy generation and thermal stability in a slab. *J Thermophys Heat Transfer*. 24:438-444.
- [6] Abiodun, O.A; Basant, K.; Jha, A.O. (2011) Entropy generation under the effect of suction/injection. *Applied Mathematical Modeling*, 35:4630-4646.
- [7] Eegunjobi, A.S; Makinde, O.D.( 2012) Combined effect of buoyancy force and Navier slip on entropy generation in a vertical porous channel. *Entropy*, 14, 1028-1044.
- [8] Adesanya S.O, Makinde O.D.(2014) Entropy generation in couple stress fluid flow through the porous channel with slippage. *International Journal of Exergy*, 15:344-362.
- [9] Makinde O.D, Eegunjobi A.S. (2013) Effects of convective heating on Entropy generation rate in a channel with permeable walls. *Entropy*, 15:220-233.
- [10] Nejib, H.; Mounir, B.; Mourad, M.; Ammar, B.B (2011) Effect of radiation heat transfer on entropy generation at thermosolutal convection in a square cavity subjected to a magnetic field. *Entropy*, 13; 1992-2012.
- [11] Samuel O.A. (2014) Second law analysis for third-grade fluid with variable properties. *Journal of thermodynamics*, article ID452168, 8pages
- [12] Srinivasacharya D, Srikanth D.(2007) Effect of couple stresses on the flow in a constricted annulus. *Arch. Appl. Mech*. 78:251-257.
- [13] Opanuga A.A, Okagbue H.I, Agboola O.O.(2017) Irreversibility analysis of a radiative MHD poiseuille flow through a porous medium with slip condition. *Proceedings of the world congress on engineering*.
- [14] Chen S, (2011) Entropy generation of double-diffusive convection in the presence of rotation. *Appl. Math.Comput*, 217, 8575-8597.
- [15] Adesanya, S.O.; Makinde, O.D.(2015) irreversibility analysis in a couple stress film flow along an inclined heated plate with the adiabatic free surface. *Physical A*, 432:222-229.
- [16] Chen S, (2011) Entropy generation of double-diffusive convection in the presence of rotation. *Appl. Math.Comput*, 217, 8575-8597.
- [17] Falade J.A, Adesanya S.O, Lebelo S.R, Kareem S.O.(2017) Second law analysis for a porous channel flow with asymmetric slip and convective boundary conditions. *International journal of applied mathematics*. 115:247-257.
- [18] Das S and Jana R.N (2014) Entropy generation due to MHD flow in a porous channel with Navier slip. *Ain Shams Eng.J*. 5, 575-584.
- [19] Adesanya S.O, Makinde O.D.(2014) Entropy generation in couple stress fluid flow through the porous channel with slippage. *International Journal of Exergy*, 15:344-362.
- [20] Makinde O.D (2011) Second Law analysis for variable viscosity hydromagnetic boundary layer flow with thermal radiation and Newtonian heating. *Entropy*, 15:220-233.
- [21] Bejan A.(1996) Entropy generation minimization: the method of thermodynamic optimization of finite-size systems and finite-time processes, CRC Press.
- [22] Zhou, J.K.(1986) *Differential Transform and its Application to Electrical Circuits*, Wuhan, Huarjung University Press.
- [23] Baoqing L, Xiaojian, Qikui D. (2015) Differential Transformation Method for some Delay Differential Equations, *Applied Mathematics*, 585-593, 6
- [24] Pukhov G.E. (1986) *Differential transformations and mathematical modeling of physical processes*, in Russian, NaukovaDumka, Kiev.
- [25] Ayaz F.(2004) Solution of the system of differential equations by differential transform method, *Applied Mathematics, and Computation*, 147:547-567.
- [26] Kurnaz A. Oturanc G. (2005) The differential transform approximation for the system of ordinary differential equations, *International Journal of Computer Mathematics*. 82:709-719.
- [27] Karako, and Berekegoglu (2009) Solutions of delay differential equations by using differential transform method. *International Journal of Computer Mathematics mathematics*, 2(3):426-447.
- [28] Guven K., Aytac A., Ebru T., Ibrahim O. (2010) Second-Law Analysis for an inclined channel containing porous-clear fluid layer by using differential transform method, *An International journal of computational and methodology* 57:8 603-623.
- [29] Che H.C.H. Adem, K, Arif, M.(2010) General Differential Transformation Method for Higher Order of Linear Boundary Problem, *Borneo Science* 27.
- [30] Rashid and Keimanesh, 2010. Using differential transform method and Pade approximant for solving MHD flow in a laminar liquid film from a horizontal stretching surface, *Mathematical Problems in Engineering* 2010, 49:1319.